# $N_2/O_2/H_2$ DUAL-PUMP CARS: VALIDATION EXPERIMENTS

S. O'Byrne[*], P. M. Danehy[†]

*NASA Langley Research Center, Hampton, VA, 23681*

A. D. Cutler[‡]

[‡]*The George Washington University, Hampton, VA, 23681*

## ABSTRACT

The dual-pump coherent anti-Stokes Raman spectroscopy (CARS) method is used to measure temperature and the relative species densities of $N_2$, $O_2$ and $H_2$ in two experiments. Average values and root-mean-square (RMS) deviations are determined. Mean temperature measurements in a furnace containing air between 300 and 1800 K agreed with thermocouple measurements within 26 K on average, while mean mole fractions agree to within 1.6 % of the expected value. The temperature measurement standard deviation averaged 64 K while the standard deviation of the species mole fractions averaged 7.8% for $O_2$ and 3.8% for $N_2$, based on 200 single-shot measurements. Preliminary measurements have also been performed in a flat-flame burner for fuel-lean and fuel-rich flames. Temperature standard deviations of 77 K were measured, and the ratios of $H_2$ to $N_2$ and $O_2$ to $N_2$ respectively had standard deviations from the mean value of 12.3% and 10% of the measured ratio.

## INTRODUCTION

Historically, a combination of one-dimensional computations, semi-empirical modeling, and the results of technology demonstration experiments has been used to design supersonic combustion ramjet (scramjet) engines that would power future hypersonic space vehicles. More recently, fully three-dimensional computational fluid dynamics (CFD) codes are instead being used.[1] These flows are turbulent, reacting, and have large regions of flow reversal. They exhibit shock waves, shock-boundary layer interactions, and other compressibility effects. Owing to these complexities, many simplifying assumptions are typically made to make the computer codes fast enough for practical engine design.

For computational efficiency, the Reynolds averaged (time averaged) form of the Navier-Stokes equations are used. This requires the introduction of empirical models for the turbulence. The chemical mechanisms in CFD codes are simplified, and chemistry-turbulence interactions are often neglected altogether. Unfortunately, many aspects of the models used in these codes are largely untested because of the lack of, and difficulty in obtaining, quantitative flowfield measurements. Though a limited database of flowfield measurements in scramjet engines exists, most previous comparisons between CFD and experiments have been limited to wall pressure, wall temperature and thrust.

Accurate flowfield data are required to validate existing models and to develop new ones.[1] The most desired measurements are temperature, major species concentrations, and velocity. A measurement system that could simultaneously measure several or all of these properties at a single point in the flow is particularly sought after. Such a system would be able to produce important correlation statistics, such as temperature-species correlations, temperature-velocity correlations and species-velocity correlations. These

[*] National Research Council Postdoctoral Fellow, Hypersonic Airbreathing Propulsion Branch, MS168, NASA Langley Research Center, Hampton, VA, 23681.

[†] Instrumentation Systems Development Branch, MS 236, NASA Langley Research Center, Hampton, VA, 23681.

[‡] The George Washington University, MS 335, NASA Langley Research Center, Hampton, VA, 23681.

correlations are particularly important for determining the numerous coefficients in the turbulence models.

This paper describes a series of calibration experiments aimed at characterizing a non-intrusive, optical system for simultaneously measuring temperature and the relative mole fractions of $N_2$, $O_2$ and $H_2$. We have used the dual-pump coherent anti-Stokes Raman spectroscopy (CARS) method.[2,3] Conventional broadband $N_2$ CARS[4] uses two spectrally-narrow green beams as pump beams and one spectrally-broad red beam as the Stokes beam. The frequency difference between the green and red beams typically corresponds to the vibrational Raman shift of $N_2$. The CARS signal is then a spectrally broad blue beam that contains the $N_2$ spectrum. This spectrum can be fit on a computer with a theoretical model to determine the temperature.

The dual-pump CARS technique used in the current work instead uses one yellow and one green pump beam. The same broadband red beam is used as in conventional broadband $N_2$ CARS. The frequency of the yellow pump beam is chosen so that the frequency difference between the yellow and red beams equals a vibrational Raman resonance of $O_2$. Thus, the resulting blue CARS spectrum contains both $N_2$ and $O_2$ spectra. The relative intensities of these two spectra provide a measure of the relative mole fractions of $N_2$ and $O_2$.

Coincidentally, several pure-rotational Raman transitions of $H_2$ are present in these spectral regions as well. These spectra are also measured in the present experiment, allowing the relative mole fractions of $N_2$, $O_2$ and $H_2$ to be quantified. Though not performed in this paper, it is possible to make assumptions about the chemistry to estimate the $H_2O$ mole fraction, based on the measured species. Under this assumption, absolute mole fractions of the four major species of hydrogen combustion can be determined.

Several different methods have been proposed for simultaneous measurement of multiple species using CARS.[4] These methods include the dual-Stokes vibrational CARS technique where two different broadband beams are used to interact with two green pump beams, generating two spatially-separated CARS signal beams. This method requires measurement of all three laser intensities and careful calibration of multiple detectors in order to determine species mole fractions from relative signal intensities. On the contrary, the dual-pump CARS method uses the same three laser beams to generate signal beams from all three different molecules. The signal beams are collinear and are all collected on the same detector. This eliminates the need for and errors associated with laser-pulse-energy measurements and detector calibrations.

Another method used to measure $O_2$ and $N_2$ simultaneously is pure-rotational CARS.[5] This method has some advantages compared to vibrational CARS performed herein, but in complicated flow environments containing many species, pure rotational CARS spectra can become very complicated with many species overlapping in the measured spectra. The dual-pump CARS method, on the other hand, allows good separation of the $N_2$, $O_2$, and $H_2$ spectra so that spectral overlaps are minimized. The major disadvantage of the dual-pump CARS method is that it produces lower signal intensity than conventional CARS by a factor of four or more, because the degeneracy of the green pump beams has been removed. This decrease in signal cannot typically be overcome by arbitrarily increasing the laser power because of well-known saturation effects that occur at higher powers. Nevertheless, dual-pump CARS has been used with success by several authors in high-speed reacting flows.[6]

**Theoretical Modeling of CARS Spectra**

The CARSFIT program,[7] developed at Sandia National Laboratories, Livermore, CA, was used to fit the data to determine temperature and species mole fractions. This program computes theoretical CARS spectra and compares them with experimental spectra to determine the best fit, using the method of least squares. Several parameters are freely adjusted to allow best fit to be obtained. These include temperature, species mole fractions and a horizontal shift in the spectrum to account for beam steering effects in the experiment that cause the signal beam to move on the detector.

In our previous work[8] we used CARSFIT to produce a library of spectra for various values of temperature and $N_2$ concentration. However, the current application of dual-pump CARS is significantly more challenging, owing to the additional fit parameters of $O_2$ and $H_2$ mole fractions. The presence of $H_2$, in particular, complicates the analysis because hydrogen spectral lines are rather narrow, causing the spectral code to increase the number of computation points dramatically (by over an order of magnitude). In addition to slowing the computation down, this also makes the required 4-dimensional (temperature, $N_2$, $O_2$, and $H_2$) quick-fitting libraries unmanageably large. Thus, for the present work, we have used CARSFIT's own internal fitting algorithm, which does not guarantee a global minimum in the least squares fitting method.

We made a few significant modifications to the CARSFIT program for the current work. We increased the array sizes to allow for computation of larger spectral regions than were previously possible, while still being able to adequately resolve the rotational hydrogen lines. This increase in array sizes slowed execution of the program but was necessary to compute $N_2$, $O_2$, and $H_2$ simultaneously. We corrected an error in the adaptive gridding option that is used to speed up the code. We also recompiled the code to run with LINUX to facilitate batch processing of the data. Finally, the dual-pump version of CARSFIT described in previous work[3] assumed that the green pump beam was monochromatic, eliminating the computation of one convolution and thereby increasing the speed of computation for each calculated spectrum. Use of an injection-seeded YAG laser in their experiment[2] also improved measurement precision compared to the use of an unseeded laser, such as that used in the current work. We have adapted the CARSFIT code to allow an additional convolution for the finite-linewidth green pump beam for the current work, though at substantial computational cost. The convolution used in the calculation of the furnace and flame spectra takes the form

$$S_{as}(\omega'_{as}) = \kappa I_1 I_2 I_{sw} \{[(\chi_{1r}^2 + \chi_{1i}^2) \otimes g_1 + (\chi_{2r}^2 + \chi_{2i}^2) \otimes g_2 + 2(((\chi_{1r} \otimes g_1)\chi_{2r} \otimes g_2 + ((\chi_{1i} \otimes g_1)\chi_{2i} \otimes g_2)] \otimes g_d\}$$

where $I$ denotes laser intensity, $\chi$ denotes the CARS susceptibility with real and imaginary parts $\chi_r$ and $\chi_i$, $g_1$ and $g_2$ represent the unity-normalized laser lineshapes of pump beams 1 and 2 respectively, and $g_d$ represents the unity-normalized instrument response function for the detection system. It is the seven convolutions, denoted by the $\otimes$ symbol, that have increased the code's execution time. This is two additional convolutions in the cross-terms that are not computed if a monochromatic pump 1 is assumed. Using the modified CARSFIT, single spectrum containing $N_2$ and $O_2$ requires around 20 seconds to calculate, and about two minutes is required to compute one spectrum containing $N_2$, $O_2$ and/or $H_2$ at flame conditions using a 1.5 GHz dual-processor Pentium IV computer operating under Linux. Fitting 200 air spectra at 1500 K required approximately 33 hours. By running multiple copies of the code on 20 different nodes of a Beowulf computer cluster, we were able to expedite processing of the entire data set. We are currently working to improve the optimization algorithm so that fewer spectral computations are required to accurately determine the best-fit parameters, reducing the time required to fit the spectra.

## EXPERIMENT

The dual-pump CARS system uses an unseeded frequency-doubled Nd:YAG laser (Spectra Physics DCR-4) which produces about 550 mJ per pulse at 532 nm. The pulse duration is about 10 ns and the repetition rate is 10 Hz. The output of the YAG laser was split three ways. Approximately 80 mJ was used as the green pump beam for CARS. A homemade, conventional broadband dye laser operating at 607 nm was pumped by 250 mJ of green light from the YAG. The dye solution contained Rhodamine 640 laser dye in methanol. The lineshape of the broadband laser was well represented by a double-Gaussian, the main Gaussian having a width of approximately 150 $cm^{-1}$, with a smaller and wider Gaussian required to adequately model the wings of the profile. This was necessary to ensure proper normalization in the wings of the spectrum, particularly when the spectrum includes strong $H_2$ lines in that spectral region. Additional details about the above components of the laser system can be found in reference 8. Finally, 200 mJ was used to pump a 574-nm narrowband dye laser (Lambda Physik, FL3002) that had been converted from excimer pumping to YAG pumping. The FL3002 dye laser oscillator beam usually reflects twice from the grating before passing to the amplifier. The second reflection is used to reduce the laser's amplified spontaneous emission (ASE). During the process of converting the FL3002 for pumping with a YAG laser, Lambda Physik recommends inserting a mirror into the grating chamber to prevent the second reflection from the grating, to prevent possible grating damage. This modification, however, causes the level of ASE to be increased markedly.

The green and red beams were combined using a dichroic mirror. All three beams were then passed through a spherical lens having a focal length of 410 mm. Planar BoxCARS phase-matching geometry was used, with the green and red beams overlapping.

The probing volume formed at the intersection of the three beams had a minimum diameter FWHM of 130 μm, measured by traversing a knife edge across the foci of all three beams, and a length FWHM of 1.8 mm, measured by traversing the probe volume across a thin planar jet of nitrogen gas, surrounded by a 30-mm-diameter jet of argon, and measuring the $N_2$ CARS signal as the probing volume was traversed across the nitrogen sheet.

A second 410-mm focal-length lens collected and collimated the three input beams as well as the blue CARS signal beam at 491 nm. Two dichroic mirrors

that efficiently reflected blue while transmitting yellow light were arranged in a multi-reflection configuration to isolate the blue signal beam. This blue beam was then directed into a one-meter spectrometer (McPherson) with a 1200 groove/mm grating. Two cylindrical lenses provided a sharp horizontal focus at the spectrometer exit for high spectral resolution. The signal was captured on a 1100x330 pixel non-intensified, back-illuminated, CCD camera (Pixel Vision, SV11CBJ). The 330-pixel region was binned into three separate rows and then read out to allow a more rapid acquisition of data. A LabView interface was created to download the spectra to a PC for subsequent analysis and to display the data in real-time for signal optimization.

When acquiring CARS spectra, several other spectra were obtained for later use in the analysis. Background scans were obtained by blocking the red laser beam and acquiring 200 spectra. These scans include contributions from camera dark noise as well as scattered green light from the room. These scans are averaged together during the analysis and subtracted from each of the CARS signal scans prior to analysis. Another measurement is performed to determine the spectrum of the broadband laser. Argon gas is flowed through a tube that encompasses the CARS measurement volume. Small holes in the tube allow the laser beams to pass through. Due to the absence of any resonant gas ($N_2$, $O_2$ or $H_2$) only nonresonant CARS signal is generated by the laser beams. This so-called 'nonresonant CARS spectrum' provides a measurement of the spectral shape of the broadband dye laser beam.

The background-corrected signal spectra are divided by background-corrected nonresonant spectra to remove the shape of the broadband dye laser from the CARS signal spectra. The nonresonant spectrum is not measured simultaneously with the resonant CARS spectra. This is unfortunate because we have used a spectrometer to observe that the broadband dye laser's spectrum shifts noticeably over time scales comparable to that of the experiment. A wavy or sloped CARS signal far from the $N_2$, $O_2$ or $H_2$ resonances provides evidence of poor normalization. We have found that shifting the nonresonant spectrum by up to 30 pixels (23 wavenumbers) can flatten the off-resonance CARS signal, providing a satisfactory normalization. In the current experiment, nonresonant spectra were shifted by eye on a run-by-run basis. The process involved examining a region of spectrum containing nonresonant signal on either side of the resonant spectrum, then shift the nonresonant spectrum until the slope of the residual between the normalized and theoretical spectra in this region was close to zero. In the future, we plan to automate this process.

Before each of the flame and furnace experiments, 200 single-shot CARS spectra were obtained in ambient air, to determine the instrument response function of the measurement system. CARSFIT was used to generate an unconvolved theoretical air spectrum. A nonlinear least-squares fit to a sum of two Gaussian distributions was used to determine the best fit between the measured experimental spectrum and the convolved theoretical spectrum. The secondary Gaussian was 6% of the size of the main response function and some 10 times wider. Use of this function produced significantly better fits to experimental data than a single Gaussian, particularly at the base of the $H_2$ peaks and the $N_2$ band head. The same instrument function would be used over the entire day's experimental data. The fitted instrument function produced consistent results over the entire range of conditions for both the furnace and flame experiments. It should be noted that it is possible that the necessity for a dual-Gaussian instrument function may have arisen because of the ASE in the narrow-band dye laser output. If this is the case, it would have been more correct to have a dual Gaussian for the pump beam convolution than for the instrument function.

Measurements were obtained in an atmospheric-pressure furnace containing air. Furnace measurements have two advantageous characteristics: the temperature can be varied independently of gas composition and the temperature can be checked against a thermocouple because the system is in radiative equilibrium. In flames, thermocouples tend to radiate at high temperatures and can produce systematically low temperature readings.

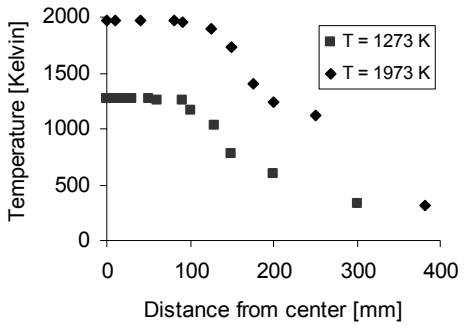


**Figure 1: Plot of spatial uniformity in the furnace for two peak temperatures.**

The furnace (Lindberg, using a West 5010 temperature controller) consisted of a resistively heated quartz tube that was capable of operation from ambient temperature up to 1973 K. However, to prevent possible thermal damage to the CARS system, we limited the temperature to 1800 K in the experiment. To make the temperature at the center of the oven more uniform, four sections of spun quartz insulation were inserted into the 7.62-cm-diameter tube. These pieces of insulation were approximately 5 cm in length and contained a 2.5-cm diameter hole in the center to allow passage of the laser beams. The four pieces of insulation were equally spaced, with the first and last pieces located adjacent to the ends of the tubes. Figure 1 shows a temperature profile in the oven obtained using a NIST-traceable type-B thermocouple. The measurements show that the temperature is very uniform over the ten centimeters outward from the center of the oven. The measurements also show that the thermocouple reading agrees with the oven's internal temperature measurement to within 5 K as long as the oven was left to stabilize for 15 minutes and the temperature of the controller was set to a value of at least 473 K. For the remainder of the experiment, the oven's internal measurement readout was used as the nominal temperature.

Measurements were also performed in an atmospheric pressure, 'Hencken' flat-flame burner using hydrogen as fuel and air as oxidizer. The flame gases were shrouded by a co-flow of helium provided to stabilize the flame. High flow rates, between 16.2 and 22.2 standard liters per minute for air and between 4.3 and 27 standard liters per minute for hydrogen, were chosen so that heat transfer to the burner surface would be minimized and the flame would be well approximated as adiabatic. The flame equivalence ratio, $\Phi$, was varied between 0.5 and 4 using Teledyne Hastings mass flow meters. The uncertainty in the equivalence ratio is estimated to be +/-3%. Measurements were obtained in the center of the 2.5-cm square burner, and at a height of 2.0 cm above the burner surface. Previous single-pump $N_2$ CARS measurements in this flame indicated that this region of the flame has a uniform spatial temperature distribution at these flow rates.

## RESULTS AND DISCUSSION

### Furnace

Figure 2 shows a comparison between temperatures measured with CARS and a thermocouple in the Lindberg furnace. The temperature in the furnace was varied between 293 K and 1773 K. Each measurement consisted of 200 single-shot CARS spectra. Fits were produced for each individual spectrum. For colder conditions, less than 1 % of fits failed to converge (the code returned the initial conditions), but this increased to 5 % for the 1773-K measurement. These results were excluded from the analysis. The error bars in figure 2 indicate the standard deviation of the individual measurements. The average standard deviation in temperature is approximately 64 K, or 3.6% of the highest measured temperature. The absolute standard deviation tends to increase with temperature.

All of the averaged measurements produce temperatures that are slightly lower than the nominal values, although all of the measurements were well within one standard deviation of the nominal temperature. The mean difference between the measured and nominal temperatures was 26 K.

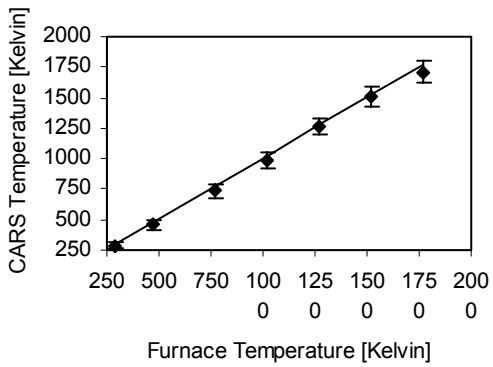


**Figure 2: CARS measured temperature in the furnace.**

To the authors' knowledge, this is the first measurement of temperature and mole fraction in a furnace using dual-pump CARS, although the technique has been extensively tested in various flame environments, as will be described in the discussion of the flat-flame results. Reference 9 describes furnace measurements using broadband $N_2$ CARS. Temperature standard deviations in these measurements were of the order of 2% at 1187 K, compared to our standard deviation of 5% at 1273 K. The reason for this discrepancy is most likely due to the use of a modeless Stokes laser in reference 9. These results are also consistent with those of reference 10, in which the temperature precision improves from 5% to 1% when a modeless dye laser replaces a conventional standing wave laser like the one used in the present measurements. Reference 11 determined that this improvement is most marked when a single-mode pump laser is used with the modeless Stokes laser.

The variations in the measured mole fractions of $N_2$ and $O_2$ are presented in figure 3. The horizontal lines correspond to the mole fractions for standard air.[12]

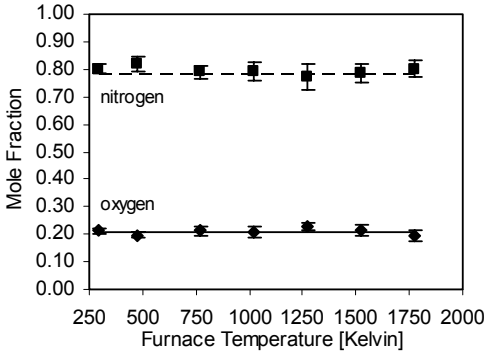


**Figure 3: Measured mole fractions of $N_2$ and $O_2$ for the furnace measurements.**

Once again the error bars on the plot indicate the standard deviation of the measurement. The average measured $N_2$ and $O_2$ mole fractions differ from the tabulated values by 1.6% and 0.4% respectively. The average standard deviations for the $N_2$ and $O_2$ mole fractions are 3.8% and 7.8% of the measured values respectively. There is no trend with changing temperature apparent in the agreement with the expected mole fractions, or with the standard deviations of either absolute mole fraction. A direct comparison can be made with the standard deviations in room-temperature air quoted in reference 3. Our measured standard deviation of 5.2% is comparable with the 4.5% quoted in that study. Reference 5 quotes similar uncertainties in a furnace using pure rotational CARS of $O_2$ at temperatures between 300 and 2050 K, and also shows no significant trends in the precision of the measurements with changing temperature.

When the dual-pump CARS technique is applied to scramjet combustor flows, the overall gas composition will not be accurately known. Under these circumstances, the nonresonant gas susceptibility cannot be determined without making additional assumptions about the chemistry. Thus, absolute mole fractions determined from CARSFIT will not necessarily be reliable. However, ratios of resonant gas species would still be reliable under these conditions. The $O_2/N_2$ mole fraction ratio is presented in figure 4. As expected from the agreement of the absolute mole fraction measurements, the relative mole fraction is consistent with expected data. The agreement is worse and the standard deviation is greater, because it is the ratio of the two measure quantities, both differing slightly from the nominal values.

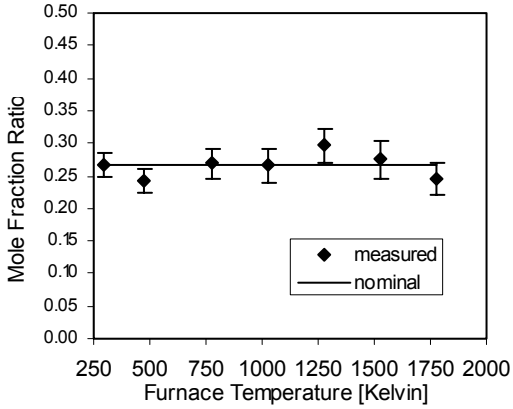


**Figure 4: Measured average $O_2/N_2$ mole fraction ratios for the furnace measurements.**

The average $O_2/N_2$ mole fraction ratio was 0.266, approximately 1% lower than the expected value of 0.2682. The standard deviation in the ratio is 0.023, or 8.7% of the measured value. There is no trend either in systematic error or in the standard deviation as the temperature varies.

**Flame**

The flame results presented here are still preliminary and only the $\Phi$ = 0.5, 1.0 and 3.0 results will be discussed here, although data at equivalence ratios of 0.75, 2.0 and 4.0 were also obtained. Figure 5 shows averaged spectra and CARSFIT fits for the $\Phi$ = 0.5 and 1.0 cases respectively. The averaged values are fitted well by the code. The $\Phi$ = 0.5 spectrum clearly shows both $N_2$ and $O_2$ bands, while the $\Phi$ = 1 spectrum does not because the oxygen has been consumed. The individual rotational lines are not resolved in the spectra. $H_2$ does not appear in either spectrum because all of the fuel has been consumed at this location in the flame. The $\Phi$ = 1 spectrum shows some rotational line structure in the first excited vibrational band. This is much easier to see in the averaged plot than in individual spectra. The $\Phi$ = 1 plot also shows a small oscillation in the data, particularly in the higher vibrational bands at the left of the plot. Although this is not easy to see in the spectrum of figure 5(b), it is visible as oscillations in the residual. This small-amplitude signal oscillation is caused by thin-film interference fringes in the CCD. If the averaged non-resonant spectrum is shifted by a few pixels, this

oscillation can be removed in the normalization of the signal to the nonresonant, which is the case for the $\Phi = 0.5$ data. This noise does not have a significant effect on the fitted temperature, but may have a significant effect on measured $O_2$ mole fraction when that quantity is small. We intend to make the non-resonant shift a fit parameter in future analysis, and this should remove the oscillations from the data.

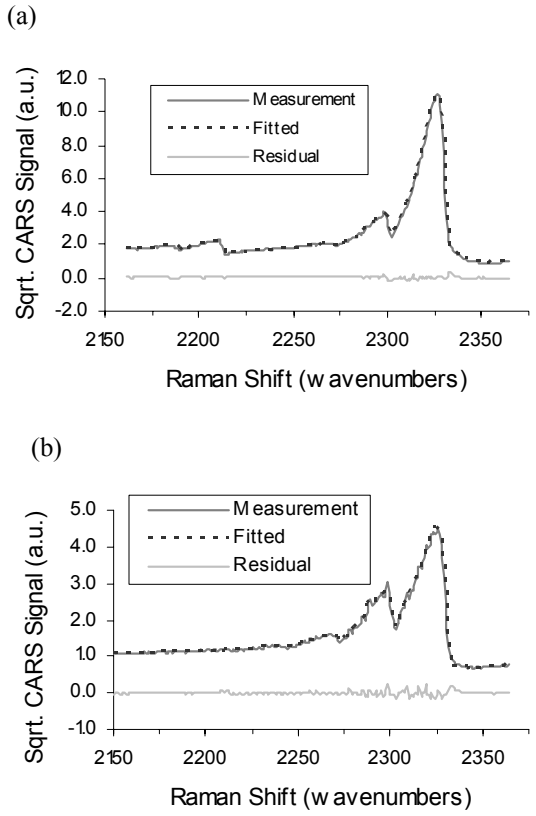


**Figure 5: Averaged spectra with fits for (a) $\phi = 0.5$ and (b) $\phi = 1.0$.**

Fit parameters for average temperature, $N_2$ mole fraction and $O_2$ mole fraction were 1575, 0.578 and 0.094 respectively for $\Phi = 0.5$ and 2270, 0.527 and 0.0 for $\Phi = 1.0$. The standard deviations in temperature for 200 individual single-shot spectra were 4.0% of the measured values in each case. The average temperature standard deviation for these two measurements was 77 K. Both measurements are about 1 standard deviation lower than the expected value for an adiabatic flame as calculated using the NASA Lewis equilibrium code[13]. The average $O_2$ mole fraction in the $\Phi = 0.5$ measurement agrees with the computed value of 0.093. The standard deviation in the ratio of $O_2/N_2$ measured in 200 single-shot spectra was approximately 10% of the measured value.

Figure 6 shows a single-shot spectrum obtained in a fuel-rich atmospheric pressure flame ($\Phi = 3.0$). Because this is a fuel-rich condition, and water is the only major non-resonant species likely to exist in the spectrum, the background non-resonant susceptibility was set to that of water for the CARSFIT calculation. The spectrum shows the $N_2$ band and also several discrete $H_2$ lines. The $O_2$ band does not appear in this spectrum because all of the oxygen has been consumed at this location in the flame. The fit parameters were 1890 K, 0.415, 0.0, and 0.337 for temperature, $N_2$ mole fraction, $O_2$ mole fraction and $H_2$ mole fraction. These parameters are the average of 62 fitted spectra. Figure 6 was chosen as a typical fit to the single-shot data. In each case the fit was good, although significant shot-to-shot variations were noticed in the relative height of the hydrogen lines. This may explain why the temperature standard deviation at this equivalence ratio, 5.7% of the measured value, is higher than for the other two flame measurements. The standard deviation in the ratio of $H_2$ to $N_2$ was 12.3% for these measurements.

The fitted temperature is significantly higher than the 1769 K adiabatic value, and the averaged fitted $N_2$ and $H_2$ mole fractions are 8.9% high and 17.6% low respectively. Reference 14 measured $H_2$ rotational CARS temperatures that were high by 70 K when compared with theory and $N_2$ CARS measurements. It may be that a similar effect is weighting the temperatures measured here, though it should be noted that the averaged $\Phi = 3.0$ spectrum produced a fitted temperature that looked like a good fit to both the hydrogen and nitrogen spectra. Another explanation

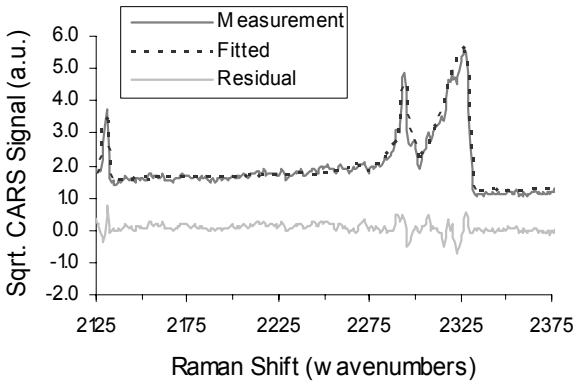


**Figure 6: Fitted single-shot $\phi = 3.0$ flame spectrum.**

that would explain both the temperature and mole fraction discrepancies is that the actual equivalence ratio is lower than expected. If the equivalence ratio of the measurement is reduced by 15%, the temperature and mole fraction measurements are brought into much better agreement with the adiabatic values. The reduction in equivalence ratio may have been brought about by incorrect flow rates due to calibration errors in the flow meters, or entrainment of surrounding air into the flame. The cause of these differences is still being investigated.

## CONCLUSIONS

Dual-pump CARS calibration measurements have been successfully performed in a furnace, and preliminary results have been obtained in a flat-flame burner. These experiments tested the technique over a range of temperatures and mole fractions of $N_2$, $O_2$ and $H_2$. Dual-pump CARS has been shown to produce consistent signals from all three species, when they are present in the flow, that can be fitted with sensible theoretical spectra. The furnace experiment produced temperatures and mole fractions consistent with thermocouple measurements and the tabulated mole fractions of $N_2$ and $O_2$ in air. Comparison with previous measurements shows results that are consistent with studies using similar apparatus and suggests that improvements to the precision of the measurements can be achieved by using a narrow-band pump laser and a modeless dye laser. Such a change would also simplify the spectral calculations. Precision is also expected to improve once the non-resonant spectrum shift is included as one of the fitting parameters.

The flame measurements, though preliminary, show agreement with theory within one standard deviation for fuel lean and stoichiometric conditions. Good fits were obtained for all three equivalence ratios chosen, with an average standard deviation of 77 K for the temperature measurements. Mole-fraction ratios had standard deviations that were 10-12% of the measured values. The mean temperature for the fuel-rich flame was systematically high by 120 K, possibly due to an overestimation of the equivalence ratio. More work is needed to determine the cause of this discrepancy.

## ACKNOWLEDGEMENTS

We wish to acknowledge the assistance of Jeff White from NASA Langley Research Center for helping analyze the CARS spectra on a large cluster of personal computers, significantly decreasing the computational time.

## REFERENCES

[1] J. P. Drummond, C. E. Cockrell, Jr., G. L. Pellett, G. S. Diskin, A. H. Auslender, R. J. Exton, R. W. Guy, J. C. Hoppe, R. L. Puster, R. C. Rogers, C. A. Trexler and R. T. Voland, "Hypersonic Airbreathing Propulsion - An Aerodynamics, Aerothermodynamics, and Acoustics Competency White Paper", NASA/TM-2002-211951, Nov. 2002. pp. 41.

[2] R. P. Lucht, "Three-Laser Coherent Anti-Stokes Raman Scattering Measurements of Two Species," Opt. Lett. 12, pp. 78-80, 1987.

[3] R.D. Hancock, F.R. Schauer, R.P. Lucht, R.L. Farrow, "Dual-pump CARS measurements of nitrogen and oxygen in a laminar jet diffusion flame," Appl. Opt. 36, pp. 3217-3226, 1997.

[4] For a more complete discussion about CARS, see A. C. Eckbreth, Laser Diagnostics for Combustion Temperature and Species (2nd Edition), Gordon and Breach Publishers, Amsterdam, The Netherlands, 1996.

[5] M. Schenk, A. Thumann, T. Seeger, and A. Leipertz, "Pure rotational coherent anti-Stokes Raman scattering: comparison of evaluation techniques for single-shot simultaneous temperature and relative $N_2$-$O_2$ concentration determination," Appl. Opt. 37, pp. 5659-5671 1998

[6] R. P. Lucht, V. V. Natarajan, C. D. Carter, K. D. Grinstead Jr., J. R. Gord, P. M. Danehy, G. J. Fiechtner, R. L. Farrow, "Dual-pump coherent anti-Stokes Raman scattering temperature and $CO_2$ concentration measurements," AIAA Journal, 41, pp. 679-686, 2003.

[7] Palmer, R. E., The CARSFT Computer Code for Calculating Coherent Anti-Stokes Raman Spectra: User and Programmer Information, Sandia National Laboratories Report SAND89-8206, Livermore, California, 1989.

[8] A. D. Cutler, P. M. Danehy, R. R. Springer, S. O'Byrne, D. P. Capriotti and R. DeLoach, "CARS thermometry in a Supersonic Combustor for CFD Code Validation", AIAA Journal, in press.

[9] J. W. Hahn, C. W. Park, and S. N. Park, "Broadband Coherent Anti-Stokes Raman Spectroscopy with a Modeless Dye Laser," Appl. Opt. 36, 6722-6728 1997.

[10] P. Snowdon. S. M. Skippon and P. Ewart, "Improved Precision of Single-Shot Temperature Measurements by Broadband CARS by use of a Modeless Laser," Appl. Opt. 30, pp. 1008-1010, 1991.

[11] D. R. Snelling, R. A. Sawchuk and T. Parameswaran, "Noise in Single-Shot Broadband Coherent Anti-Stokes Raman Spectroscopy that Employs a Modeless Dye Laser", Appl. Opt. 33, pp. 8295-8301, 1994.

[12] A. D. McNaught and A. Wilkinson, "IUPAC Compendium of Chemical Terminology", Blackwell Science, 1997.

[13] S. Gordon and B. J. McBride, "Computer Program for Calculation of Complex Chemical Equilibrium Compositions, Rocket Performance, Incident and Reflected Shocks and Chapman-Jouguet Detonations," NASA SP-273, NASA, Washington D.C., 1976.

[14] R. D. Hancock, K. E. Bertagnolli and R. P. Lucht, "Nitrogen and Hydrogen CARS Temperature Measurements in a Hydrogen/Air Flame Using a Near-Adiabatic Flat-Flame Burner," Combustion and Flame, 109, pp. 323-331, 1997.